JCI insight

RESEARCH ARTICLE

Guaiacol as a drug candidate for treating adult polyglucosan body disease

Or Kakhlon,[1] Igor Ferreira,[2] Leonardo J. Solmesky,[3] Netaly Khazanov,[4] Alexander Lossos,[1] Rafael Alvarez,[5] Deniz Yetil,[6] Sergey Pampou,[7] Miguel Weil,[3,8] Hanoch Senderowitz,[4] Pablo Escriba,[5] Wyatt W. Yue,[2] and H. Orhan Akman[9]

[1]Department of Neurology, Hadassah-Hebrew University Medical Center, Jerusalem, Israel. [2]Structural Genomics Consortium, Nuffield Department of Clinical Medicine, University of Oxford, Oxford, United Kingdom. [3]Cell Screening Facility for Personalized Medicine, Department of Cell Research and Immunology, The George S. Wise Faculty of Life Sciences, Tel Aviv University, Tel Aviv, Israel. [4]Department of Chemistry, Bar Ilan University, Ramat Gan, Israel. [5]Laboratory of Molecular Cell Biomedicine, Department of Biology, University of the Balearic Islands, Palma de Mallorca, Spain. [6]Connecticut College, Newington, Connecticut USA. [7]Columbia University Department of Systems Biology Irving Cancer Research Center, New York, New York, USA. [8]Laboratory for Neurodegenerative Diseases and Personalized Medicine, Department of Cell Research and Immunology, The George S. Wise Faculty for Life Sciences, Sagol School of Neurosciences, Tel Aviv University, Ramat Aviv, Tel Aviv, Israel. [9]Columbia University Medical Center Department of Neurology, Houston Merritt Neuromuscular diseases research center, New York, New York, USA.

Adult polyglucosan body disease (APBD) is a late-onset disease caused by intracellular accumulation of polyglucosan bodies, formed due to glycogen-branching enzyme (GBE) deficiency. To find a treatment for APBD, we screened 1,700 FDA-approved compounds in fibroblasts derived from APBD-modeling *GBE1*-knockin mice. Capitalizing on fluorescent periodic acid–Schiff reagent, which interacts with polyglucosans in the cell, this screen discovered that the flavoring agent guaiacol can lower polyglucosans, a result also confirmed in APBD patient fibroblasts. Biochemical assays showed that guaiacol lowers basal and glucose 6-phosphate–stimulated glycogen synthase (GYS) activity. Guaiacol also increased inactivating GYS1 phosphorylation and phosphorylation of the master activator of catabolism, AMP-dependent protein kinase. Guaiacol treatment in the APBD mouse model rescued grip strength and shorter lifespan. These treatments had no adverse effects except making the mice slightly hyperglycemic, possibly due to the reduced liver glycogen levels. In addition, treatment corrected penile prolapse in aged *GBE1*-knockin mice. Guaiacol's curative effects can be explained by its reduction of polyglucosans in peripheral nerve, liver, and heart, despite a short half-life of up to 60 minutes in most tissues. Our results form the basis to use guaiacol as a treatment and prepare for the clinical trials in APBD.

Introduction

Glycogen storage disorders. Glycogen is a branched polysaccharide with a molecular weight of nine to ten million Daltons. The average glycogen molecule contains about 55,000 glucosyl residues linked by α-1,4 (92%) and α-1,6 (8%) glycosidic bonds (1). Glycogen synthesis is catalyzed by the actions of 3 enzymes: (a) glycogenin (GYG), the initiating enzyme that starts a primer of glucose chain attached to itself; (b) glycogen synthase (GYS), which strings glucose to extend linear chains; and (c) glycogen-branching enzyme (GBE), which attaches a short new branch to a linear chain. Glycogen is stored primarily in liver and muscle; in liver, it serves mainly to keep normal glycemia and in muscle it acts as a so-called high-octane source of energy for strenuous exercise.

Diseases involving glycogen imbalance are called glycogen storage disorders (GSDs). There are 15 GSDs: some are lethal in infancy or childhood and others start later and progress slowly; however, all GSDs significantly decrease the quality of life. Genetically, most GSDs are inborn errors of metabolism caused by deleterious mutations in genes encoding enzymes involved in glycogen synthesis or breakdown. The GSDs of impaired glycogen synthesis are type 0 (GYS deficiency), type IV (GBE deficiency) and type

Conflict of interest: OK and HOA are listed authors on patent WO2017120420, which pertains to this work and is now in national phase.

Submitted: January 8, 2018
Accepted: July 31, 2018
Published: September 6, 2018

Reference information:
JCI Insight. 2018;3(17):e99694.
https://doi.org/10.1172/jci.insight.99694.

XV (GYG deficiency). Examples of impaired glycogen breakdown include glycogen-debranching enzyme deficiency (GSD type III), myophosphorylase deficiency (GSD type V), and defects in glycolysis (phosphofructokinase deficiency, GSD type VII). However, GSDs are not limited to the defects in enzymes that control the synthesis and breakdown of glycogen. For instance, in Lafora disease (LD), deficiencies in an E3 ubiquitin ligase (malin) or a phospho-tyrosine/glycogen phosphatase (laforin) also cause abnormal glycogen accumulation similar to that found in GSD type IV (GBE deficiency) (2, 3). A subgroup of GSDs also involve the insoluble inclusions polyglucosan bodies (PGBs). These pathologically diverse diseases — the adult neurodegenerative disorder adult polyglucosan body disease (APBD), the child liver disease Andersen disease (AD), the adolescent epilepsy LD, and the myopathy Tarui disease (TD, type VII GSD [phosphofructokinase deficiency]) — all manifest accumulation of the presumably pathogenic PGB, which contains malconstructed insoluble glycogen.

At present, there is no treatment for GSDs except for acid maltase deficiency (GSD II, Pompe disease), where the defective lysosomal acid maltase can be replaced by a genetically engineered enzyme. However, enzyme replacement works only for deficiency of lysosomal enzymes, because lysosomes have a unique protein uptake mechanism mediated by mannose 6-phosphate receptors.

GSD type IV. GSD type IV (OMIM 232500) can have a very early infant onset (in AD) or a late adult onset (in APBD) (4). AD is an autosomal recessive disorder caused by deficiency of GBE and leads to the accumulation of polyglucosan in liver, heart, skeletal muscles, and the central nervous system. Polyglucosan causes liver cirrhosis or cardiopathy or, rarely, a pure myopathy (5). APBD, on the other hand, is a neurodegenerative disorder that simulates amyotrophic lateral sclerosis (ALS), but is often associated with bladder dysfunction and — in about 50% of patients — with dementia. It is indeed difficult to explain the clinical heterogeneity between AD and APBD; however, it seems to depend on the relative extent of GBE activity. The complete loss of GBE activity in AD is fatal in infancy and the degree of residual GBE activity seems to determine the age at onset and type of the disease (infant in AD or adult in APBD).

Treatment of APBD by GYS inhibition. The late-onset and residual GBE activity in APBD imply that there is a therapeutic window in which the disease can be treated. Potential strategies can be aimed at either boosting glycogen branching activity or clearing the accumulated polyglucosan. Another strategy is to inhibit glycogen synthesis by inhibiting GYS activity — either GYS1 expressed in all tissues but the liver, or GYS2 uniquely expressed in the liver. In fact, downregulating glycogen synthesis would seem to be a good solution for all glycogenoses, regardless of their different mechanisms and clinical prognoses. Recent publications have supported the validity of this approach (1, 6, 7). However, the absence of glycogen inflicts a large burden on the energy need of a newborn. In fact, only 5% to 10% of newborn pups survive in the GYS1-knockout mouse model (8). However, those that survive live normal lives and only have moderate heart problems caused by hypoglycemia in late-adult life. In mouse models it has been shown that deficiency of GYS1 can be tolerated after birth and curative to GSD as long as hypoglycemia is kept in check. *GYS1* knockdown in LD-modeling *Epm2a*$^{-/-}$ mice led to complete rescue of the murine LD phenotype in mice up to the age of 2 years; PGB was no longer formed, there was no neurodegeneration, and the myoclonic epilepsy disappeared (6). Partial reduction of GYS was also therapeutic in mice. *Epm2a*$^{-/-}$ and *Epm2b*$^{-/-}$ LD mice in which protein targeting to glycogen (PTG), a protein that activates GYS by inducing its dephosphorylation (9), was knocked out and reduced the GYS activity by 50% completely rescued LD (10, 11). Similarly, in malin-deficient mice heterozygous for *Ptg*, i.e., mice with an anticipated 25% reduction in glycogen synthesis, there was a dramatic reduction of the abnormal brain glycogen accumulation characteristic of LD and over 50% reduction in myoclonus (10, 11). Similar results were also obtained for APBD-modeling mice homozygous for the human p.Y329S mutation (Berge Minassian, unpublished observations).

Clinical reports suggest that this phenomenon is also true in humans; all patients with *GYS1* mutations were young children, who, if they did not die suddenly during exercise, developed normally (12, 13). If GYS1 deficiency in humans is as life-threatening as in mice, probably most newborns with severe *GYS1* mutations die early in infancy or succumb to sudden infant death syndrome. However, the data show that in humans, complete absence of GYS1 is compatible with life, with the exception of cardiac disease, and is not associated with brain disease. The parents of patients with complete GYS1 deficiency have 50% GYS activity and are completely healthy (12). Likewise, complete absence of GYS2 is compatible with life, with the exception of overnight-fasting hypoglycemia, a condition readily treatable with nocturnal nasogastric tube feeding. Again, heterozygous parents of these patients are healthy (13).

Therefore, as it is evident that substantial therapeutic benefit of GSD occurs with partial, even modest, reductions in glycogen synthesis, we aimed to find a pharmacological way to partially inhibit GYS activity in adults with GSD type IV (APBD) who have surmounted neonatal hypoglycemia and lived normal lives without the complications of glycogen storage until a certain age where PGBs were large enough to cross a certain quantitative threshold and become pathogenic (i.e., cause APBD).

Guaiacol — a GYS inhibitor and a candidate for APBD therapy. Initially used for treating lung abscesses (14), guaiacol has been used to treat reflux esophagitis (15) and, in combination with codeine (Pulmo Bailly), or as a precursor to guaifenesin (Resyl Syrup), to treat cough. In this work, we show that guaiacol, discovered as a positive hit for PGB reduction in a high-throughput screening (HTS) campaign, is a potent, nontoxic inhibitor of GYS1 and GYS2. Our data further suggest that the guaiacol-associated GYS1 phosphorylation is a part of a general catabolic stimulation, as AMP-dependent kinase (AMPK), which is the master switch that activates cell catabolism, was also phosphorylated and activated by guaiacol. We showed that guaiacol can inhibit purified GYS1 and GYS2 in vitro, as corroborated for GYS1 by computational active-site-docking analysis. Kinetically, we have confirmed that guaiacol is a competitive inhibitor of purified GYS1 and GYS2 and a mixed inhibitor of the enzymes in cell lysates.

Our studies on guaiacol treatment of an APBD mouse model are encouraging, as the drug reduced heart, liver, and (most importantly) peripheral nerve polyglucosans and significantly restored the short lifespan of *GBE1*-knockin mice ($GBE1^{ys/ys}$, where both copies of the *GBE1* gene contain the human p.Y329S mutation; ref. 16) to normal, without any significant adverse effects. In conclusion, guaiacol seems to be a promising drug for treating APBD and other PGBs involving GSDs with minimal side effects.

Results

Discovery of guaiacol as a therapeutic candidate for APBD. In our hands, guaiacol, initially used for treating respiratory and throat ailments (14, 15), was discovered as a drug candidate for APBD by HTS of the 1,700-compound library of FDA-approved drugs (Supplemental File 1; supplemental material available online with this article; https://doi.org/10.1172/jci.insight.99694DS1). This HTS was performed in fibroblasts derived from APBD-modeling mice ($GBE1^{neo/-}$) (17), which are compound heterozygous, with a polymorphic allele and exon 7 deletion, in their GBE. This HTS tested whether candidate compounds can lower the levels of diastase-resistant, periodic acid–Schiff–positive (PAS-positive) inclusion bodies, operationally defined as polyglucosans (Figure 1). Normal cells do not have PGB accumulation and give very light background, unlike $GBE1^{neo/-}$ cells. When we compared WT to mutated cells, the *Z*-factor was 0.9. When we subtracted the background, the *Z*-factor became 0.98 (Figure 1, A and B). Guaiacol treatment decreased the PGB staining but did not abolish it completely.

When tested on mouse embryonic fibroblasts (MEFs) (Figure 2, A and B, dose escalation shown in C) and fibroblasts derived from APBD patients (Figure 2D), guaiacol demonstrated the best dose-response profile in comparison to other polyglucosan-reducing hits, such as mitotane, terpin, and benzbromarone. For that reason, we decided to continue our studies with guaiacol.

Guaiacol increases the phosphorylation of GYS1. GYS1 (nervous system and muscle form) is an allosteric enzyme that can be activated by glucose 6-phosphate (G6P) or inactivated by phosphorylation of serine residues on the enzyme (18). Therefore, we have checked the phosphorylation status of GYS1 in muscle extracts as an indicator of its activity. Figure 3 shows that the phosphorylation of GYS1 increased with guaiacol treatment. This increase was assessed by normalization of the phosphorylated GYS1 signal to intrinsic total GYS1 protein. GYS1 protein amount in tissue did not change significantly by the guaiacol treatments. Since guaiacol abruptly increased GYS1 phosphorylation at 45 mg/kg administered to mice, we further tested lower concentrations of 22.5, 12, and 6 mg/kg and found that 22.5 mg/kg in drinking water is the lowest effective guaiacol concentration in terms of the other parameters tested.

Guaiacol increases AMPK phosphorylation and reduces available energy. Glycogen synthesis and breakdown is regulated according to the energy state of the cell determined by the ratio of ATP to ADP. When glucose is abundant the amount of ATP is higher and that of AMP is low so that AMPK remains unphosphorylated and inactive. However, when glucose concentrations are low ATP production decreases, while ATP is converted to ADP and AMP by cellular processes that use ATP as an energy source. Higher concentrations of ADP and AMP activate AMPK, or, more specifically, its α subunit (AMPKα) (19). Active AMPKα triggers catabolic metabolism, which prevents the synthesis of glycogen, lipids, and most proteins while activating glycogen breakdown, oxidative phosphorylation, and mitochondrial biogenesis. Therefore, in

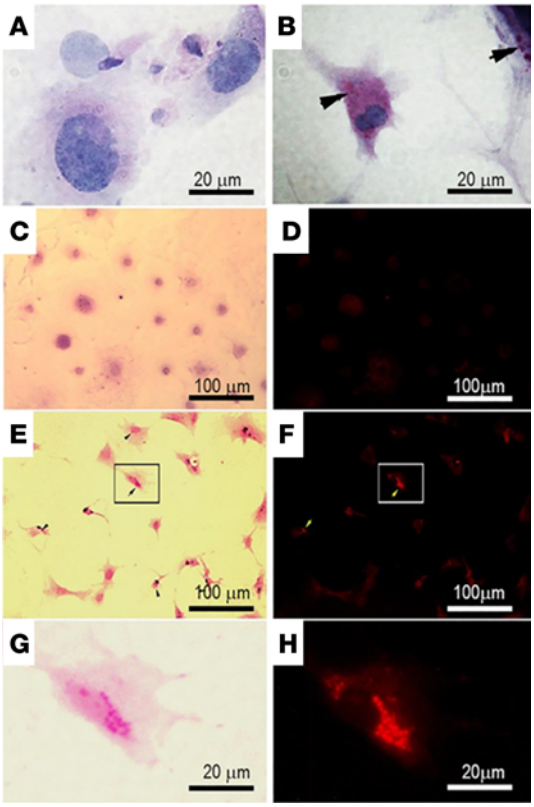

Figure 1. Diastase-resistant PAS-positive accumulations in *GBE1*$^{neo/-}$ mouse embryonic fibroblasts (MEFs) are detectable by light microscopy as well as fluorescence microscopy. (**A**) *GBE1*$^{+/+}$ cells do not exhibit periodic acid–Schiff–positive (PAS-positive) staining in the cytosol. (**B**) *GBE1*$^{neo/-}$ fibroblasts accumulate polyglucosan bodies (PGBs), indicated by arrowheads (×600 magnification). (**C** and **D**) PAS-stained control MEFs with lower magnification (×200) and fluorescence image of the same field. (**E** and **F**) The same imaging technique was used to detect PGBs (black and yellow arrowheads) in *GBE1*$^{neo/-}$ MEFs. (**G** and **H**) Digital magnifications of the outlined fields in **E** and **F** showing large round PGBs. Scales of each image are indicated in the bottom right corner. Representative images out of hundreds taken during the HTS campaign.

order to evaluate the effect of guaiacol on overall energetic status, we tested its effect on the state of AMPK phosphorylation in muscle extracts.

As shown in Figure 4A, guaiacol treatment increased the phosphorylation of AMPKα Thr172, which is an indicator of its activation. Total AMPKα protein levels were not affected by guaiacol. The activation of AMPKα by guaiacol is in line with its phospho-inhibitory action on GYS1 (Figure 3) and with a catabolic shift in cell metabolism. Since increased AMP versus ATP can activate AMPKα, where the active site resides, we measured AMP, ADP, and ATP levels in muscle extracts. While there was no significant difference in total adenosine levels between WT and *GBE1*$^{ys/ys}$ (the APBD-knockin mouse model homozygous for the human mutation; ref. 16), both in guaiacol-treated and untreated mice, guaiacol treatment led to a significant decrease in adenosine levels in both WT ($P < 0.02$) and *GBE1*$^{ys/ys}$ ($P < 0.03$) mice (Figure 4B). This decrease in overall adenosine levels by guaiacol represents a global energetic deficit, possibly compensated by attenuation of glycogen synthesis by GYS1.

Guaiacol inhibits GYS1 activity. We performed a series of experiments aimed at unraveling guaiacol's mode of action. The most likely endogenous target, whose inhibition is expected to lower polyglucosan accumulation, is GYS1 (nervous system and muscle isoform). GYS1 elongates glycogen chains and might therefore lead to polyglucosan formation when GBE-mediated branching of these chains is deficient. As guaiacol induces GYS1 phosphorylation (Figure 3), which can inhibit the enzyme, we tested whether guaiacol also decreases GYS1 activity. These experiments tested GYS1 basal as well as G6P-stimulated activity and were conducted with purified GYS1 and in cell lysates of APBD patient fibroblasts expressing GYS1. The results, using both purified enzyme and lysate (Figure 5), show that guaiacol inhibited both basal and G6P-stimulated GYS1 activity.

The effect of guaiacol on GYS1 activity was also addressed using recombinant GYS1 that was coexpressed with glycogenin (GYG1). As an indicator of GYS1 activity, we assayed glucose chain elongation on the GYG1-GYS1 complex using PAS staining. As purified GYG1-GYS1 complex already had a glucose chain attached to GYG1 (likely during recombinant expression), as indicated by the purple stain on SDS-PAGE gel (Figure 6A, 0 mM UDP-glucose [UDPG]). Adding the glucose donor, UDPG, allows GYS1 to elongate the glucose chain in GYG1, as indicated by the upward shift in purple stain (Figure 6A, 0.1–2 mM UDPG). When added at 100-fold excess of UDPG, guaiacol prevents glucose chain elongation in

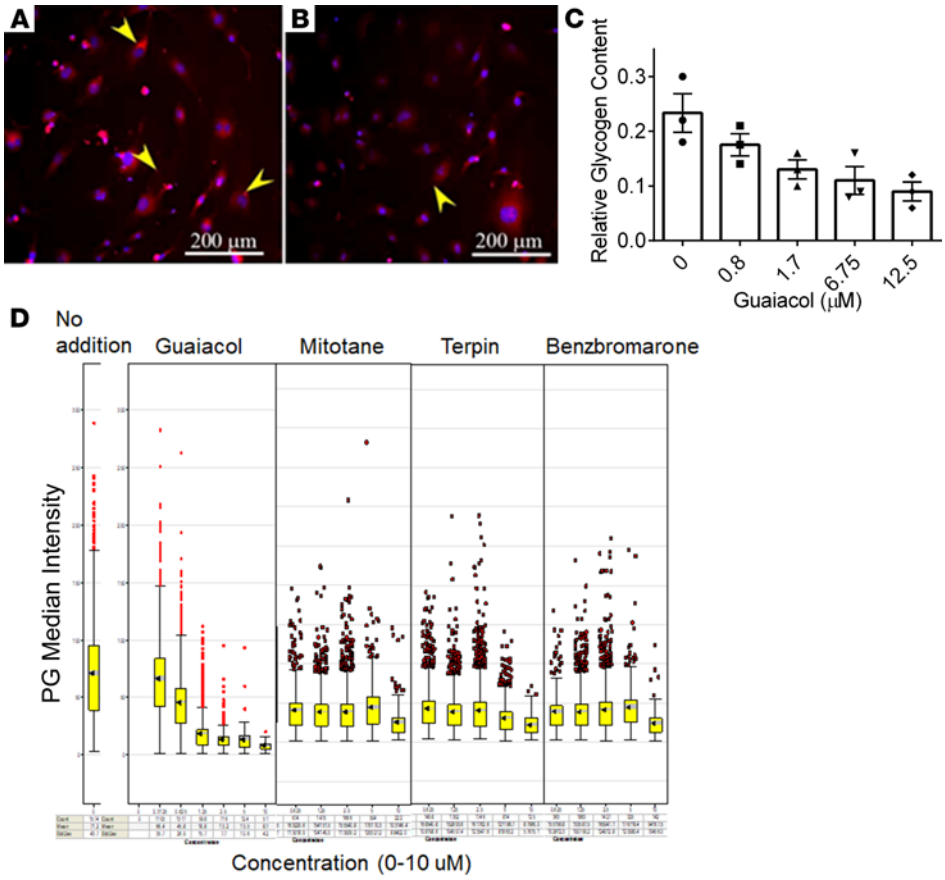

Figure 2. Guaiacol decreases polyglucosan and glycogen synthesis. (**A**) Diastase-treated periodic acid–Schiff–stained (PAS-stained) mouse embryonic fibroblast (MEF) cultures. (**B**) Guaiacol (10 μM) treatment decreased PAS-stained polyglucosan bodies in the cytosol, indicated by yellow arrow heads in **A** and **B**. (**C**) Decrease of glycogen content in MEFs (n = 3) grown in cobalt-supplemented media after 3 days of guaiacol treatment at concentrations indicated on the horizontal axis. Nonlinear regression analysis predicted IC50 of 6.8 μM (F test, $P < 0.0001$). (**D**) Box-and-whisker plots depicting the effect of concentration on diastase-resistant, cell-associated, median PAS fluorescence intensity in APBD patient fibroblasts treated for 24 hours with the indicated compounds at the indicated concentrations. Arrowheads indicate median PAS intensity. The yellow boxes delineate upper and lower quartiles from the median, and upper and lower whiskers, respectively, show maximal and minimal PAS intensity values. Red dots denote outliers with values at least 1.5 × (interquartile range [75th percentile – 25th percentile]) above or below the box. Nonlinear regression analysis predicted IC50 of 0.9 μM for guaiacol (F test, $P < 0.0001$).

the GYG1-GYS1 complex (Figure 6B). The effect of guaiacol was dose dependent (Figure 6C), and was not directed towards GYG1 (W.W. Yue, unpublished observations). Altogether, our data demonstrate that guaiacol can inhibit GYS1 activity in vitro.

The GYS1 active site can accommodate guaiacol. In vitro or in lysates the GYS1 inhibition results might be explained by increased GYS1 phosphorylation (Figure 3), which inhibits both basal GYS1 activity and its affinity towards G6P (20). With purified protein, without kinases, the inhibition cannot involve phosphorylation. Therefore, the fact that guaiacol inhibited the activity of recombinant GYS1 in buffer (Figure 5), where kinases are unavailable, suggests that its mode of action is competitive with respect to UDPG. This hypothesis was supported by our in silico studies using a yeast homolog of GYS1 (Figure 7). This analysis shows that guaiacol can be docked to the GYS1 active site, adopting a binding mode which overlaps with the glucose moiety of UDPG, thus supporting binding competition between guaiacol and UDPG.

Guaiacol is a competitive inhibitor of purified GYS1 and a mixed inhibitor of the enzyme in cell lysate. The fact that guaiacol increases GYS1 phosphorylation (Figure 3) argues against a competitive inhibitory mechanism and supports a noncompetitive mode of inhibition, in contrast to the computational prediction based on a purified protein. We therefore carried out a kinetic analysis in order to resolve this issue. Figure 8 shows that guaiacol is a competitive inhibitor of GYS1 when using a purified enzyme, but a mixed

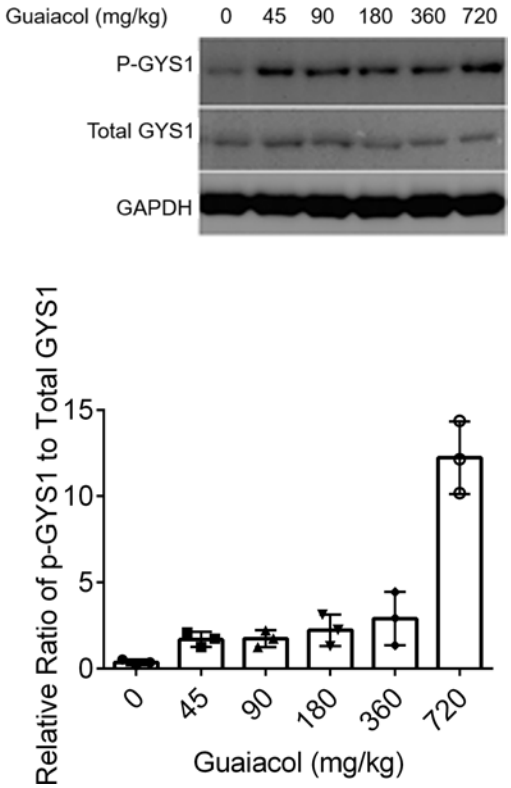

Figure 3. Guaiacol increases the phosphorylation of glycogen synthase. Western blot analysis of phosphorylated glycogen synthase 1 (p-GYS1), total GYS1, and glyceraldehyde 3-phosphate dehydrogenase (GAPDH) as a control for protein loading, in muscle extracts obtained from WT mice 2 hours after guaiacol treatment. Animals were given water-dissolved guaiacol in drinking water at the amounts indicated in the top panel. Guaiacol significantly increased GAPDH-normalized p-GYS1 to total GYS1 ratios at all concentrations ($n = 3$, $P < 0.05$, Student's t test).

inhibitor in cell lysate. These data are in agreement with data obtained in the *GBE1*$^{ys/ys}$ mice of GYS1 phosphorylation and AMPK activation (Figures 3 and 4, GYS1 is an AMPK substrate) and with the in silico–predicted docking of guaiacol to the active site (Figure 7). The location of guaiacol in the binding site of GYS1 is similar to that of the phosphoglucose moiety of UDPG (Figure 7A). UDPG forms a total of 10 hydrogen bonds in the binding cavity: 5 hydrogen bonds with the backbone of Gly42, Trp512, Tyr514 (2 hydrogen bonds), and Thr512 and 5 hydrogen bonds with the side chain of the residues Lys39, Arg331, Tyr493, Tyr514, and Glu518 (Figure 7C). In addition, the positively charged Arg331 forms a salt bridge with the negatively charged oxygen of the phosphate group of UDPG. This bonding pattern is different from that of the phosphate group in UDP (Figure 7B). Guaiacol forms 1 hydrogen bond with the backbone of Trp512 and 2 hydrogen bonds with the backbone of Gly513 (Figure 7D). Residue Trp512 participates in the interactions with both UDPG and guaiacol.

In summary, in lysate both competitive and noncompetitive inhibition might take place as guaiacol can both lead to GYS1 phosphorylation and displace UDPG. In buffer, however, without kinases, guaiacol can only competitively inhibit GYS1. As can be observed in Figure 8 and Table 1, in lysate guaiacol both decreased V_{max} and increased K_m (Figure 8A) and in buffer it only increased K_m (Figure 8B).

Guaiacol reduces tissue glycogen content in the liver and polyglucosan content in the liver, heart, and peripheral nervous system. We observed a significant decrease in liver glycogen in mice treated with guaiacol. However, glycogen content in the brain, heart, and muscle did not change significantly (Figure 9). Polyglucosan was affected by guaiacol in the same way as glycogen content in MEFs (Figure 2, A–C) and APBD patient-derived cells (Figure 2D). In tissues (Figure 10), polyglucosan was reduced in the liver and peripheral nerves, and to some extent in the heart. These observations are in accordance with guaiacol acting as a GYS inhibitor; reduction of GYS1 activity (Figures 5, 6, and 8) can explain the decreases in glycogen and polyglucosan levels in MEFs and APBD fibroblasts (Figure 2), and polyglucosan levels in MEFs, APBD fibroblasts (Figure 2), peripheral nerve, and heart (Figure 10). On the other hand, guaiacol-mediated inhibition of GYS2 activity, kinetically similar to the inhibition of GYS1 activity (Figures 11 and 12 and Table 2), can explain the decreases in glycogen and polyglucosan content in the liver (Figures 9 and 10, respectively). The fact that, despite its inhibitory effect on GYS1 and GYS2, guaiacol did not affect glycogen and polyglucosan in the same way in all tissues suggests that factors in addition to intrinsic GYS inhibition can determine guaiacol-mediated reduction of tissue glycogen and polyglucosan. Of these putative factors, we decided to focus on pharmacokinetics.

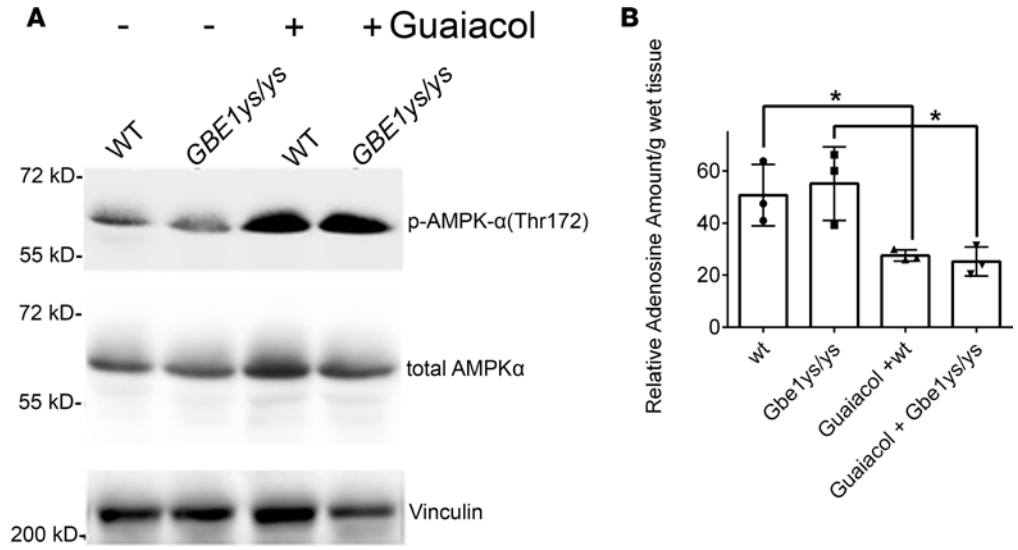

Figure 4. Guaiacol activates AMP kinases and decreases adenosine. Muscle extracts obtained from WT, *GBE1*$^{ys/ys}$, and 1-month-treated WT and *GBE1*$^{ys/ys}$ mice were subjected to SDS-PAGE and immunoblotted with phospho-AMP kinase α (p-AMPKα) (Thr172) and total AMPK antibodies. (**A**) Total AMPKα protein levels were used for estimating the relative phosphorylation of AMPKα. (**B**) High performance liquid chromatographic analysis of adenosine in muscle extracts. Averages and SD of $n = 3$ experiments are shown. *$P < 0.03$ by Student's t test.

Pharmacokinetics of guaiacol. One way to explain the differential effects of guaiacol on glycogen/polyglucosan content in the different tissues concerns its differential distribution and dwell time in each respective tissue. To that end, we have explored the pharmacokinetics of guaiacol in different tissues. As can be observed in Figure 13, guaiacol is relatively quickly absorbed in the kidney and muscle. This relatively fast absorption is expected in a rapidly perfused organ such as the kidney, and less expected in the muscle tissue, which is perfused more slowly. However, several factors besides perfusion, such as tissue partition coefficient and lipid solubility, tissue pH, and more, might also affect tissue absorption. Therefore, the relatively fast muscular absorption is probably also explained by factors other than perfusion. Liver and spleen show slower absorption (time to C_{max}) than muscle and kidney, possibly due to enhanced initial metabolism. However, guaiacol dwell time in the liver is longer than in the muscle, which might (at least partially) explain why glycogen and polyglucosan were reduced by the drug in the liver and not in other tissues. The heart demonstrates low levels of guaiacol. However, those levels persist, which might account for the moderate reduction in polyglucosan content observed in the heart (Figure 10). The brain, on the other hand, demonstrates only negligible accumulation of guaiacol, in agreement with lack of effect of the drug on the brain glycogen (Figure 9) and polyglucosan (Figure 10) content. The half-lives of guaiacol (from C_{max}) can be estimated as 10 minutes (kidney), 30 minutes (muscle), 30 minutes (spleen), 60 minutes (liver), and 220 minutes (heart). Low guaiacol levels in the brain hinder half-life estimation in the tissue.

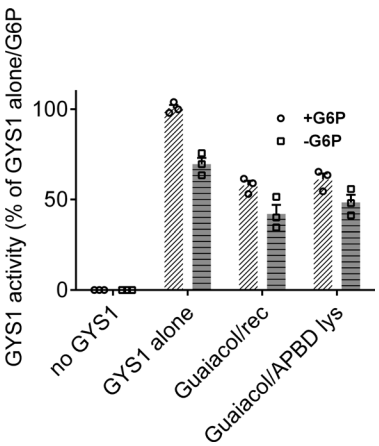

Figure 5. Guaiacol decreases biochemical activity of glycogen synthase 1 (GYS1). GYS1 activity assayed by an established radioactive assay based on incorporation of UDP-^{14}C-glucose. Where indicated, assays were performed in the presence of 10 μM guaiacol. Rec = experiment using 10 nM recombinant GYS1; lys = experiment using lysate of APBD patient fibroblasts. Raw data of $n = 3$ repetitions and respective means and SEM are shown. *$P < 0.05$ versus respective untreated control (+G6P or –G6P), based on 1-way ANOVA with Dunnet's post hoc test.

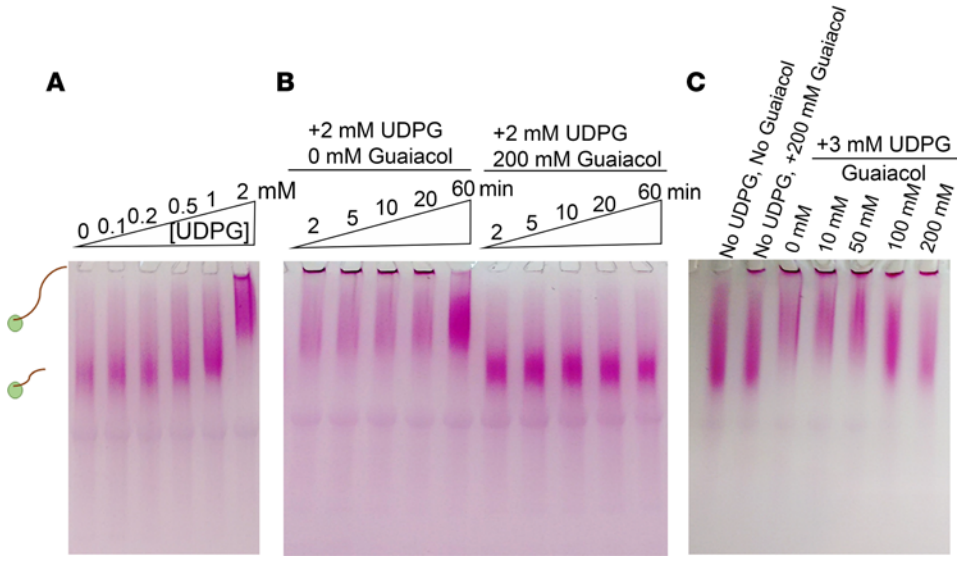

Figure 6. Guaiacol inhibits glycogenin 1–linked glycogen synthase 1 (GYS1) activity. (**A**) Glucose chain elongation of recombinant glycogenin 1 (GYG1)-GYS1 complex analyzed by SDS-PAGE and stained with periodic acid–Schiff's reagent (PAS). The upward shift in stain with increasing UDPG concentration indicates formation of higher-MW glucose chain. (**B**) Over the course of 60 minutes, guaiacol inhibits the upward shift in stain for the GYG1-GYS1 complex, indicative of an inhibition of glucose chain elongation. (**C**) Concentration-dependent effect of guaiacol on the PAS staining. A representative experiment repeated 3 times.

Guaiacol reduces glucose tolerance. Consistent with guaiacol-mediated GYS inhibition, blood glucose levels following postfasting glucose administration were increased in both guaiacol-treated control and *GBE1*$^{ys/ys}$ mice (Figure 14). This reduced glucose tolerance is expected following administration of a GYS inhibitor.

Guaiacol increases the lifespan of GBE1$^{ys/ys}$ *mice*. We treated mice with guaiacol in drinking water for 12 months every other day by preparing fresh guaiacol solution in water. The discovered effective dose of 22.5 mg/kg did not adversely affect the animal behavior, as concluded from grip test (Figure 15) and weight gain or losses, which were not different from untreated groups (Supplemental Tables 1 and 2). *GBE1*$^{ys/ys}$ mice normally live for 12 months (16). However, guaiacol-treated *GBE1*$^{ys/ys}$ mice lived for up to 24 months (Figure 16A), the time at which we sacrificed the animals as required by our protocol. Other obvious benefits of the guaiacol treatment in male mice were that it (a) reversed penile prolapse (Figure 16B), a condition observed in untreated mice starting at age as early as 1 year, and (b) reduced the deterioration of 4-paw grip strength (Figure 15).

Guaiacol improves the 4-paw grip strength in GBE1$^{ys/ys}$ *mice*. Four-paw grip strength evaluated by the grip test showed significant weakness in untreated *GBE1*$^{ys/ys}$ mice at around 100 days of age. Guaiacol treatment slowed the deterioration. After 260 days of treatment, the treated animals had significantly stronger grip strength (1.65 ± 0.1 newtons) than untreated littermates (1.4 ± 0.18 newtons) (Figure 15).

Discussion

Initial discovery of guaiacol as a drug candidate for treating APBD. The amount of glycogen in normal tissues other than muscle and liver is limited and cannot be detected easily. In these tissues, glycogen is either synthesized much less or used much faster than in other tissues. To study glycogen metabolism and glycogen-protein interaction in cell culture, certain modifications are required. For example, Jiang et al. used a cell line stably transfected with rabbit muscle GYS to study the colocalization of glycogen with starch-binding domain–containing protein-1 (21). They showed that starch-binding domain–containing protein-1 targets glycogen to lysosomes. However, with regards to polyglucosan accumulation, such an approach might be problematic since increasing GYS activity also causes polyglucosan accumulation because it alters the delicate GYS/GBE activity ratio in favor of GYS. Higher GYS activity leads to the synthesis of longer unbranched chains of glycogen and therefore to the formation of diastase-resistant starch-like polyglucosan (22). Thus, we had to develop a screening method that can detect polyglucosan directly, without GYS manipulation, and can be applied in a high-throughput format amenable to the screening of multiple small molecules for their influence on polyglucosan levels. This method, applied both to MEFs and APBD

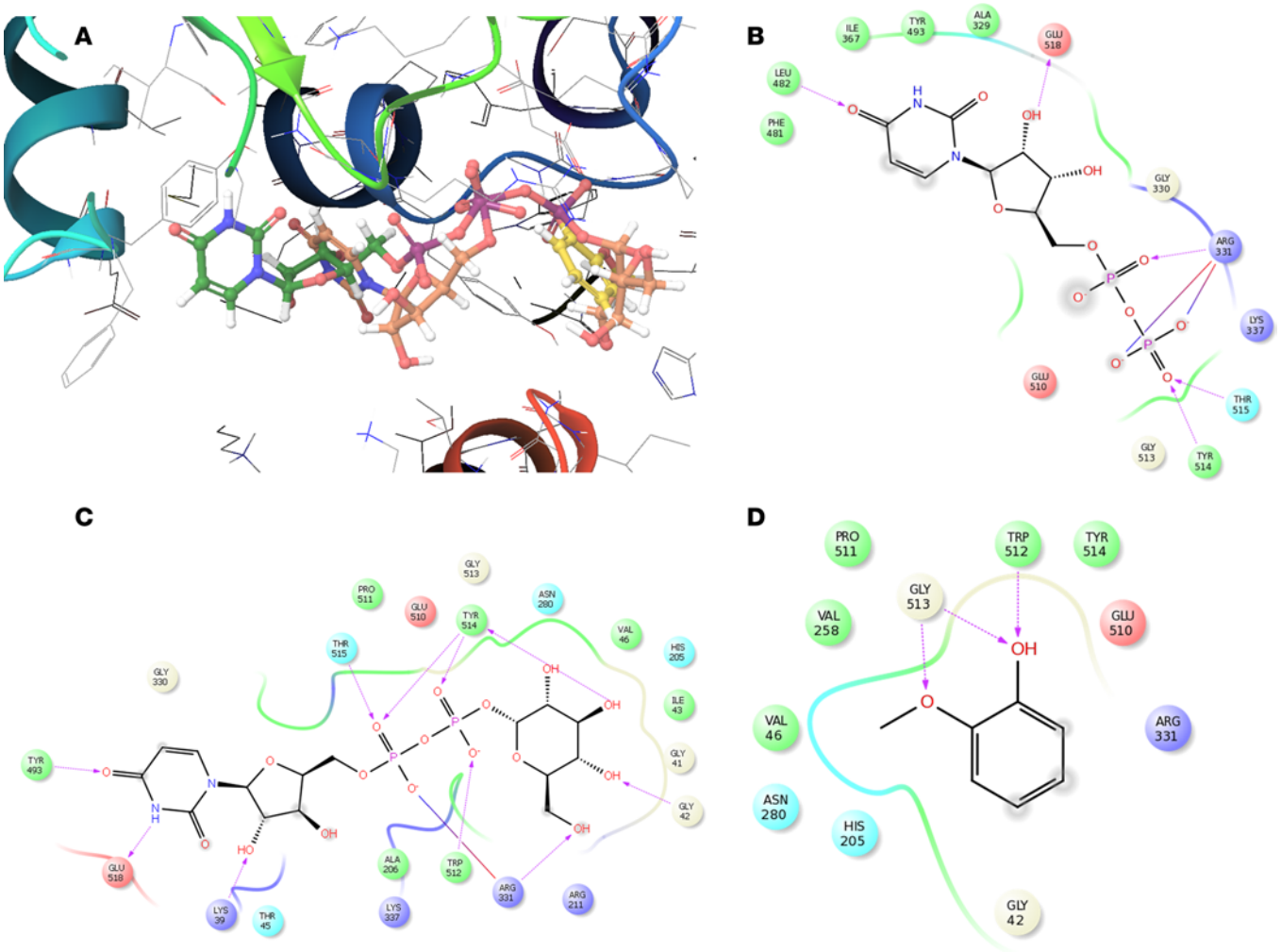

Figure 7. Glycogen synthase 1 binding models. (**A**) Docking results (Glide, SP) of UDP (green carbon), UDP-glucose (UDPG, brown carbon), and guaiacol (yellow carbon) into the UDP-binding site of a homology model of human glycogen synthase 1 (GYS1). (**B**) Binding mode of UDP (GlideScore = −5.7 kcal/mol). (**C**) Binding mode of UDPG (GlideScore = −8.0 kcal/mol). (**D**) Binding mode of guaiacol (GlideScore = −5.0 kcal/mol). Red, blue, and green spheres represent positively charged, negatively charged, and hydrophobic residues, respectively. Hydrogen bonds are presented as pink arrows in the 2D presentation.

patient–derived skin fibroblasts, was based on the operational definition of polyglucosan as an entity that can be stained by PAS and be insensitive to digestion by the glycogen-digesting enzyme diastase (up to certain ceiling concentrations and exposure times). Guaiacol was discovered by this screening assay, which capitalized on phenotypic selection of hits based on a single readout (cell-associated polyglucosan mean intensity), which can be influenced by multiple factors. Thus the observed compound effect in the analyzed images does not necessarily reveal whether the drug candidate is acting as a GYS inhibitor, GBE stabilizer, or by somehow promoting polyglucosan degradation. The observation that the mode of action of guaiacol is, at least in part, inhibition of GYS activity (Figures 5, 6, and 8) stands to reason given that GYS is the only enzyme capable of forming, during glycogen synthesis, the α1-4 interglucosidic bonds that constitute polyglucosan. Since glycogen accumulation in the cell is very limited, we used a MEF cell line with very low GBE activity. This cell line produces polyglucosan that is retained in the cell and can be detected by PAS staining. Using this cell line, we searched the Johns Hopkins University Clinical Compound Library containing 1,700 FDA-approved and foreign entity–approved drugs. The library is assembled in 384-well plate format carrying 5 mM stocks of drugs. Our search has found that guaiacol significantly decreases both glycogen accumulation and polyglucosan (Figure 10). As it is well known, molecules discovered by animal models are not always well translated to human therapy (23). Thus, we have also confirmed a guaiacol effect and, moreover, the dose dependence of this effect, in APBD patient–derived skin fibroblasts (Figure 2D). This discovery increases the chances of translation to therapy.

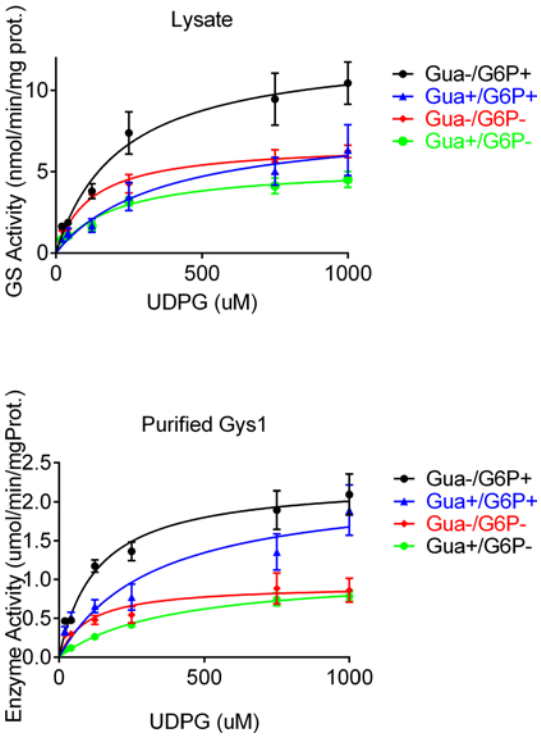

Figure 8. Guaiacol inhibits glycogen synthase 1 (GYS1) activity competitively and by a mixed model. (**A**) Results of assays using lysates from APBD patient fibroblasts suggesting that both competitive and noncompetitive inhibition might occur. (**B**) Results of assays suggesting that, in the absence of kinases, guaiacol can only competitively inhibit purified GYS1. UDPG, the GYS substrate UDP-glucose. Results from $n = 3$ experiments are shown. Statistical analysis is presented in Table 1.

GYS downregulation by guaiacol as a novel strategy for treating GSDs. Irrespective of the mechanism of polyglucosan formation in the PGB-involving GSDs (APBD, AD, LD, and TD, type VII GSD [phosphofructokinase deficiency]), in the end, only GYS can generate polyglucosans, and therefore without GYS, there would be no polyglucosans. Therefore, discovering a PGB inhibitor that is also a GYS inhibitor is expectable. Another issue is the extent of GYS1 inhibition. As our data show, guaiacol is a relatively mild GYS1 inhibitor, with an estimated EC50 of more than 10 μM (Figures 5 and 10C), depending on the entity being measured (GYS activity with or without G6P, glycogen content, or, when EC50 is much higher, overexpressed GYG1-GYS1 protein, which is at relatively high levels [Figure 6]). Partial reduction of GYS activity can in fact be even more beneficial therapeutically; complete GYS inhibition might lead to sudden death mostly associated with cardiac disease (8, 12). For example, rapamycin, a potent inhibitor of both GYS activity (by 70%) and PGB accumulation (24) and of glycogen in mice modeling the GSD Pompe disease (25), was toxic to our

Table 1. Kinetic parameters (K_m and V_{max}) of guaiacol-treated and untreated purified GYS1 enzyme and APBD patient fibroblasts

	V_{max} ± SD (μmol/min/mg protein)	K_m (μM) ± SD
lys $Gua^-/G6P^+$	12.66 ± 0.93	223.0 ± 49.03
lys $Gua^+/G6P^+$	8.14 ± 1.13	365.9 ± 129.0
lys $Gua^-/G6P^-$	6.71 ± 0.30	120.9 ± 19.36
lys $Gua^+/G6P^-$	5.34 ± 0.31	201.0 ± 36.77
rec $Gua^-/G6P^+$	2.27 ± 0.11	131.5 ± 23.47
rec $Gua^+/G6P^+$	2.23 ± 0.33	328.9 ± 127.5
rec $Gua^-/G6P^-$	0.93 ± 0.08	100.7 ± 31.09
rec $Gua^+/G6P^-$	1.09 ± 0.07	383.7 ± 61.44

lys, cell lysates from APBD fibroblasts; rec, 10 nM recombinant GYS1; Gua, guaiacol (10 μM); G6P, glucose 6-phosphate (10 mM). With or without G6P, guaiacol led to significant differences between V_{max} and K_m values when added to cell lysates, and to significant differences between K_m values only when added to recombinant GYS1 protein. Significance was determined by the extra-sum-of-squares F test.

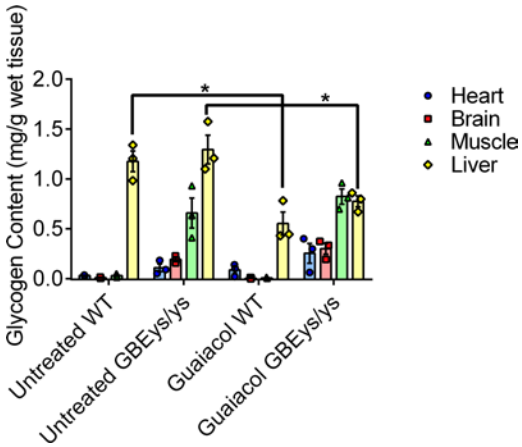

Figure 9. Guaiacol inhibits glycogen synthesis in liver, brain, heart, muscle, and liver. Glycogen content in WT, *GBE1*$^{ys/ys}$, and guaiacol-treated WT and *GBE1*$^{ys/ys}$ mice. Glycogen was measured after a 16-hour fast (n = 4 for each treatment). Glycogen content is expressed as mg/gram fresh tissue. Error bars represent the mean ± SD. *P < 0.05 by Student's t test.

APBD-modeling mice (H. Orhan Akman, unpublished observations), probably due to its pleiotropic effects. Such effects are indeed expected, as a very potent GYS inhibitor may not only reduce normal glycogen levels to below a threshold where they can be toxic; such an inhibitor might also interfere nonspecifically with the activity of other glycosyl transferases, therefore affecting protein and lipid glycosylation with the expected adverse consequences. Thus, the discovery of guaiacol as both a PGB reducer and a mild GYS inhibitor is promising in terms of future regulation and therapeutic application not only to APBD but also to the other PGB-involving GSDs — AD, LD, and TD. Interestingly, the majority of PGB reducers recently discovered by us in another APBD patient cell–based HTS (26) were also mild GYS inhibitors.

Regulatory considerations for the implementation of guaiacol as a drug for APBD and other GSDs. Guaiacol is a naturally occurring substance derived from wood creosote and present in wood smoke. Being an FDA-approved food supplement, guaiacol is used as a flavoring and aromatic agent and is found, for instance, in

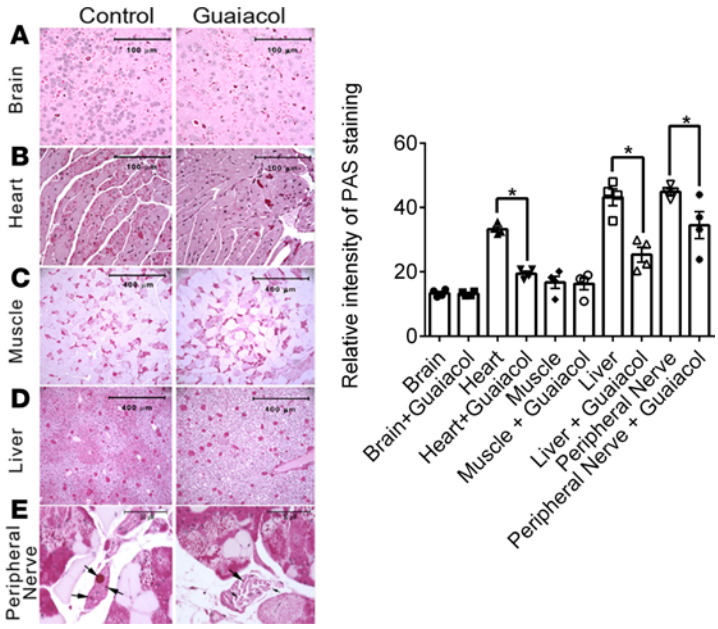

Figure 10. Guaiacol treatment decreases the amount of polyglucosan in heart, liver, and peripheral nerves. (**A**–**E**) Representative periodic acid–Schiff staining (see Methods) of polyglucosan in guaiacol-treated (left panel) and untreated (right panel) tissues from *GBE1*$^{ys/ys}$ mice. Tissue is indicated to the left of the panel. Note smaller polyglucosan bodies in guaiacol-treated animals (**E**). (**F**) Quantification of PAS staining based on n = 4 experiments. *P < 0.05 by Student's t test (following guaiacol treatment).

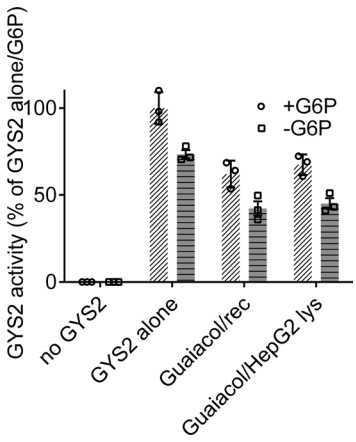

Figure 11. Guaiacol decreases biochemical activity of glycogen synthase 2 (GYS2). GYS2 activity assayed by an established radioactive assay based on incorporation of UDP-^{14}C-glucose. Where indicated, assays were performed in the presence of 10 μM guaiacol. Rec = experiment using 10 nM recombinant GYS2; lys = experiment using lysate of the liver cell line HepG2, which expresses the GYS2 isoform. Raw data of n = 3 experiments and respective means and SEM are shown. GYS2 activities in all guaiacol treatments were significantly reduced ($P < 0.05$) versus respective untreated control (+G6P or –G6P), based on 1-way ANOVA with Dunnet's post hoc test.

roasted coffee and vanilla. Medically, it has been used for treating respiratory diseases, cough, and reflux (14, 15). The combination of the precedential usage of guaiacol in the clinic and the encouraging in vitro and in vivo results presented here anticipate a relatively uncomplicated transition of guaiacol to clinical settings. However, further studies are still required to establish a robust pharmacokinetic profile for guaiacol in humans. The only study in which guaiacol levels in the blood were determined was a pharmacokinetic study that did not address efficacy (27). In that study, 32 mg (0.4 mg/kg, assuming average weight of 80 kg) was administered orally to patients. After 30 minutes, guaiacol level in the serum was less than 0.04 mg/l, suggesting a relatively high extraction ratio in the liver, which is also supported by our data showing relatively long dwell time in that organ.

Clinical implications. Our mouse studies on guaiacol show that the drug restored the significantly shorter lifespan of *GBE1*$^{ys/ys}$ mice to normal levels, without any adverse effects. In contrast, guaiacol corrected penile prolapse in aged *GBE1*$^{ys/ys}$ male mice, a urologic problem, which perhaps could be related to other urologic problems found in patients. As PGBs were reduced by guaiacol in peripheral nerves and as peripheral neuropathy is a major pathological component in APBD, we believe guaiacol is a promising therapeutic for the

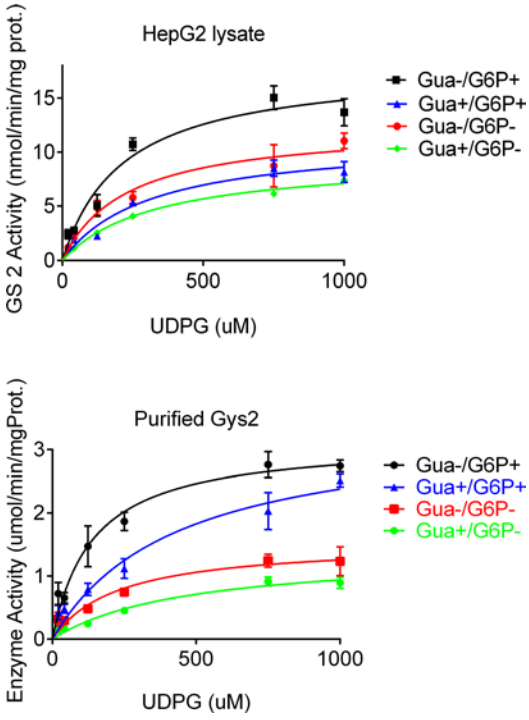

Figure 12. Guaiacol inhibits glycogen synthase 2 (GYS2) activity competitively and by a mixed model. (**A**) Results of assays (n = 3) using purified GYS2 enzyme and lysates from the liver cell line HepG2. (**B**) Results of assays (n = 3) using purified GYS2 enzyme. UDPG, the GYS substrate UDP-glucose. Statistical analysis is presented in Table 2.

Table 2. Kinetic parameters (K_m and V_{max}) of guaiacol-treated and untreated purified GYS2 enzyme and HepG2 cells

	V_{max} ± SD (μmol/min/mg protein)	K_m (μM) ± SD
lys Gua⁻/G6P⁺	18.00 ± 1.54	216.8 ± 54.49
lys Gua⁺/G6P⁺	11.29 ± 1.21	313.7 ± 89.90
lys Gua⁻/G6P⁻	12.45 ± 1.45	229.4 ± 78.91
lys Gua⁺/G6P⁻	9.44 ± 0.53	332.3 ± 48.52
rec Gua⁻/G6P⁺	3.15 ± 0.16	140.0 ± 24.25
rec Gua⁺/G6P⁺	3.40 ± 0.36	433.0 ± 109.1
rec Gua⁻/G6P⁻	1.54 ± 0.13	228.8 ± 57.16
rec Gua⁺/G6P⁻	1.38 ± 0.13	471.4 ± 107.5

lys, cell lysates from HepG2 cells; rec, 10 nM recombinant GYS2; Gua, guaiacol (10 μM); G6P, glucose 6-phosphate (10 mM). With or without G6P, guaiacol led to significant differences between V_{max} and K_m values when added to cell lysates, and to significant differences between K_m values only when added to recombinant GYS2 protein. Significance was determined by the extra-sum-of-squares *F* test.

disease. Furthermore, the guaiacol-mediated reduction of glycogen and PGB in the liver suggest that the drug might be a potent therapeutic also for AD. The very low levels of guaiacol observed in human sera (27) suggest that guaiacol might have a high extraction ratio and may therefore be considerably more effective if administered intravenously (instead of orally). A possible complication is the reduced glucose tolerance observed in guaiacol-treated mice (Figure 14). Nevertheless, this phenomenon, unexpected since guaiacol activated the GLUT4 (glucose transporter) stimulating factor AMPK, is probably manageable if replicated in guaiacol-treated patients in the future. In summary, normalization of lifespan (Figure 16A), correction of penile prolapse (Figure 16B), and improvement of muscle strength at an advanced stage of the disease (Figure 15), all without adverse effects, strongly suggest guaiacol as a potential therapeutic for APBD.

Methods

Cell cultures. MEFs were cultured in DMEM media supplemented with 10% fetal bovine serum and 1% antibiotic-antimycotic (Gibco Life Technologies). Cells were kept in a tissue culture incubator maintaining 37°C and 10% CO_2 in a humidified atmosphere.

HTS. We plated 500 cells per well in 384-well plates. The Johns Hopkins University Clinical Compound Library is assembled in seven 384-well plates carrying 5 mM stocks of drugs. We used 21 plates (3 replicates × 7) in total. Cells were grown for 2 days in growth media and then the media were changed to serum-free media supplemented with 1% antibiotic-antimycotic and 100 μM cobalt chloride. Plates were then transferred to a Cell::Explorer (PerkinElmer). This automated system with an anthropomorphic robotic arm transports microtiter plates from one module to another. On the third day, cells were treated with the chemical library by the Freedom EVO 200 (Tecan), a liquid handling system for HTS. This system is also a robotic platform that includes units for managing microplates, liquid handling, incubation, and compound library hosting. Plates were incubated for 3 more days in this machine and on the seventh day

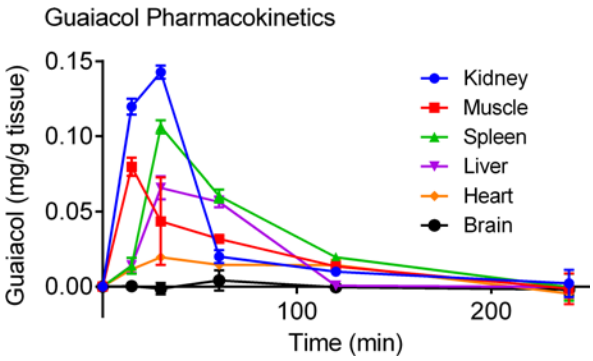

Figure 13. Pharmacokinetics of guaiacol. *GBE1*$^{ys/ys}$ mice were treated with guaiacol via oral gavage as specified in Methods. Mice were sacrificed at several time points as shown and the indicated tissues were removed. Graph shows guaiacol levels in the different tissues determined spectrophotometrically as described in Methods. Shown are means and SEM of results obtained from $n = 3$ mice. Repeated-measures 2-way ANOVA tests show that the pharmacokinetic profile of each tissue is significantly different from that of all other tissues ($P < 0.05$).

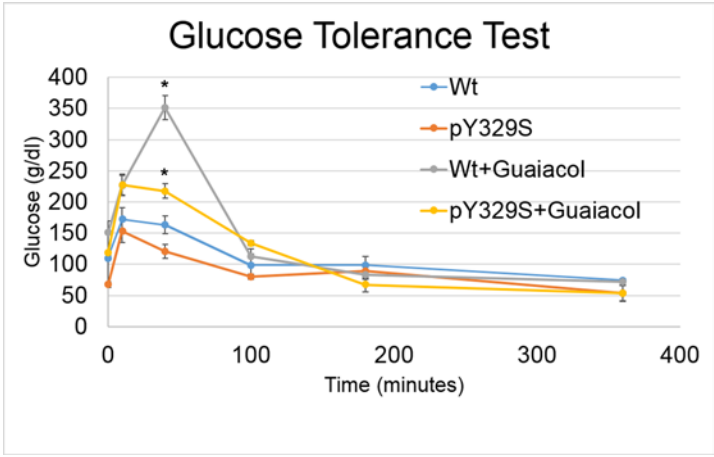

Figure 14. Guaiacol increases blood glucose concentration. Glucose tolerance test. *GBE1*$^{ys/ys}$ and control mice treated as indicated were starved overnight followed by feeding with 6 g/kg D-glucose. Blood glucose levels were measured at the indicated time intervals (n = 3). *Significantly higher blood glucose levels were observed in guaiacol-treated animals as compared with untreated ones (P < 0.01 by Student's t test).

washed in phosphate-buffered saline (PBS) and fixed in 4% formalin overnight at 4°C. The next day, cells were washed with acid/ethanol solution (95% ethanol, 5% glacial acetic acid), washed again with PBS and treated with 0.5% α-amylase type VI-B (Sigma-Aldrich) for 20 minutes, washed with PBS, and treated with 0.5% periodic acid for 30 seconds. Then cells were washed with water and stained with Schiff's reagent for 10 minutes, washed twice with 0.55% potassium metabisulphite and tap water. Cells were counterstained with 4,000-fold diluted Hoechst stain in PBS for 10 minutes and washed with water. The cells were then covered with 90% glycerol/10% PBS. Fluorescence images were taken with an IN Cell Analyzer 2000 (GE Healthcare) using a ×10 lens and analyzed with an image analysis protocol developed using the Multi-Target Analysis module of the IN Cell Analyzer Workstation (GE Healthcare). PGB staining of APBD patient–derived skin fibroblasts was done as previously described (26).

SDS-PAGE and Western blotting. Standard protocols were employed for Western blotting. Briefly, muscle tissue was homogenized 3 times in sample buffer (62.5 mM Tris-HCl [pH 6.8 at 25°C], 2% w/v SDS, 10% glycerol, 50 mM DTT, 0.01% w/v bromophenol blue or phenol red), quantified by the Lowry method, and 10 mg protein was separated on SDS-PAGE. Proteins were transferred to PVDF membranes by Mini Trans-Blot apparatus (Bio-Rad). After transfer, membranes were blocked with 3% milk in TBST. After 1 hour of blocking at room temperature, membranes were immunoblotted with p-GYS1, GAPDH, p-AMPKA, AMPKA, vinculin (Cell Signaling Technology, respective catalog numbers 3891, 5174, 4188, 2793, and 13901), and GYS1 (Abcam, ab40810) antibodies, according to the suppliers' protocols.

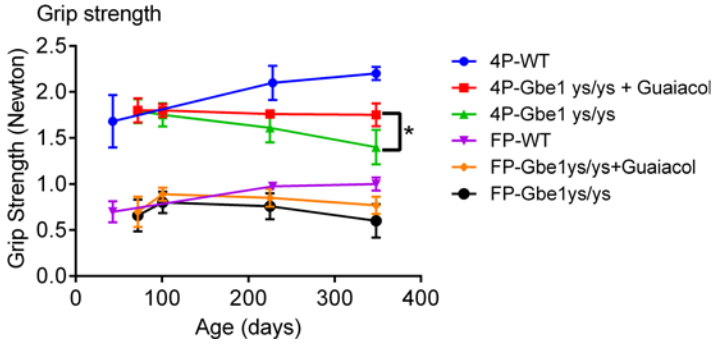

Figure 15. Guaiacol treatment improves the grip strength in *GBE1*$^{ys/ys}$ mice. Two- to 12-month-old guaiacol-treated animals showed slower decrease in neuromuscular function compared with untreated littermates assessed by the grip test. Data are expressed as force in newtons ± SD (error bars) of at least 5 animals per group. *P < 0.05 by Student's t test. FP, front paw; 4P, four paw.

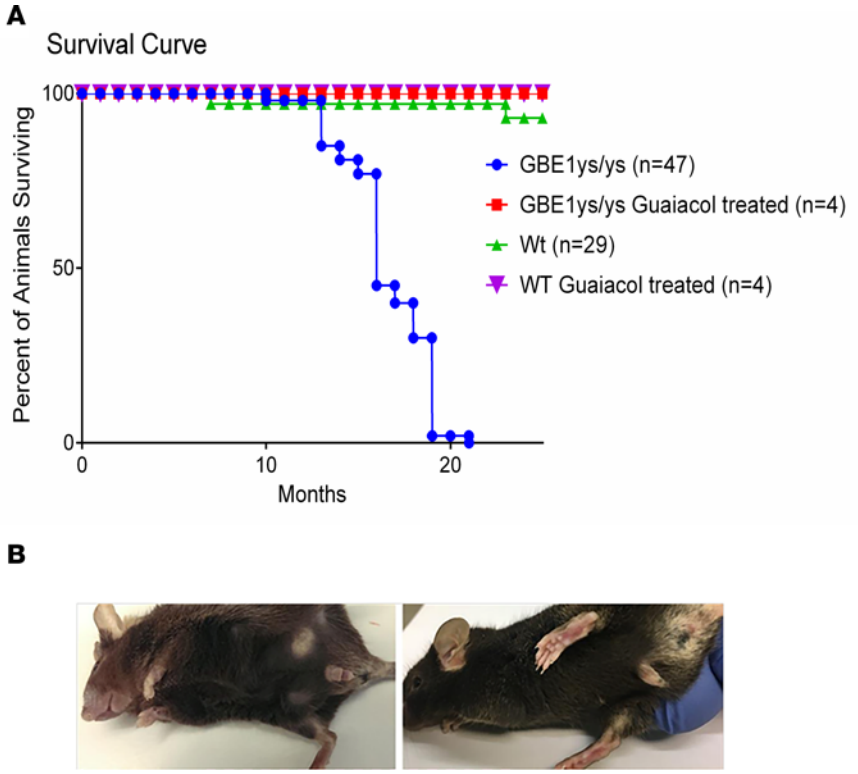

Figure 16. Guaiacol treatment extends the lifespan of the *GBE1*$^{ys/ys}$ mice and cures penile prolapse. (**A**) Kaplan-Meier plot illustrates the incidence of death in *GBE1*$^{ys/ys}$ (n = 47), versus WT mice (n = 29) and guaiacol-treated *GBE1*$^{ys/ys}$ and WT mice (n = 4 each). (**B**) Penile prolapse is prevented by guaiacol treatment. Untreated mouse on the left exhibits penile prolapse compared with the treated mouse on the right. Images representative of observations in at least 10 aged male mice.

Animals. The *GBE*$^{ys/ys}$ mouse colony was derived from the AB2.2 strain, at Baylor College of Medicine as described by Akman et al. (16). Mice were backcrossed to C57BL/6J for 10 generations and continued to be bred in the homozygous state for more than 6 generations, which makes them congenic. Congenic WT and homozygous *GBE1*$^{ys/ys}$ mice were kept at the Columbia University Medical Center animal facility (12-h light/dark cycle at a temperature of 18°C–23°C and 40%–60% humidity) before they were assigned to the study. In all animal studies described herein, 5 or fewer male mice were housed in a single cage. Food and water were provided ad libitum. The diet used was Teklad Global diet 2918 for rodents (Harlan Laboratories). Low ionic strength high-pH drinking water was refreshed twice weekly.

Animal treatments. Guaiacol was provided in drinking water at 84.4 mg/litter, which provides 22.5 mg/kg guaiacol for a 30-gram mouse that consumes 8 ml water daily (28). Water was changed every other day to ensure that the mice received fresh, unoxidized guaiacol.

Grip strength. We measured grip strength by using a Grip Strength Meter (Columbus Instruments) on guaiacol-treated and untreated *GBE1*$^{ys/ys}$ and WT mice, with at least 4 mice in each group. Forelimb grip strength was measured by allowing the mice to grip the bar with forepaws; after mice gripped the bar they were gently pulled by their tail until they lost their grip. Pulling force indicated by the Grip Strength Meter was recorded. Four-paw grip strength was measured by allowing the mice to grip a rectangular grid with all 4 limbs, followed by pulling the mice until they lost their grip; 3 force measurements in each test were recorded in each separate trial.

GYS activity assay. GYS activities using cell lysates from APBD patient fibroblasts expressing GYS1, HepG2 cells (ATCC) expressing GYS2, and purified GYS1 and GYS2 were determined based on the rate of ^{14}C-UDPG incorporation into exogenous glycogen (17).

Homology modeling of human GYS1. The yeast GYS protein (PDB code 303C) in complex with UDP is the closest homolog to human GYS1, with a sequence identity of 52.3%. This value is considered appropriate for homology modeling (29).

Pairwise sequence alignment between the 2 proteins was performed using the ClustalW tool as implemented in Discovery Studio (DS) version 4.1 with default settings. Most of the residues that participate in interactions with UDP in its binding site are conserved between human GYS1 and yeast GYS, except that Val367 is changed to Ile. The resulting sequence alignment was used as input to the MODELLER program as implemented in DS. The highest ranked model, based on the Dope scoring function, was found to have good stereochemical qualities, with 96.6% of residues residing in the most favored and additionally allowed regions of the Ramachandran plot. Template/target RMSD based on Cα atoms was 1.13Å.

Docking. Prior to the docking, the human homology model of GYS1 was prepared using the protein preparation wizard implemented in Maestro. Proper protonation states were assigned to all residues by using the Probka program at pH 7.0. The lowest-energy poses obtained with Glide SP (single precision) successfully reproduced the crystallographically observed binding mode of UDP in 303C with an RMSD of approximately 2 Å, the main difference being the location of the diphosphate group. Compounds for docking were prepared using LigPrep as implemented in Maestro with the OPLS 2005 force field in order to obtain correct protonation states and possible tautomeric states. The UDP site of GYS was subjected to SP Glide docking.

Polyglucosan staining. Brain, heart, muscle and liver tissues were fixed overnight at room temperature in 4% buffered formalin. The next day, tissues were transferred to 70% ethanol and embedded in paraffin overnight at 80°C. Paraffin blocks were sectioned at 5-μm thickness by microtome. Sections were deparaffinized and incubated with 0.5% diastase in buffer for 5 minutes at room temperature.

Tissue staining and histochemistry. Tissue sections were prepared from treated and untreated mice, fixed in 10% formalin, and embedded in paraffin. Sections (5 μm) were deparaffinized, and 1 slide of each sectioned block was treated with 40 ml of 5 mg/ml α-amylase (Sigma-Aldrich) for 25 seconds in a microwave oven set to 600 watts. Slides were then washed with deionized water and oxidized with 0.5% periodic acid for 5 minutes, stained with Schiff reagent for 15 minutes, and then counterstained in hematoxylin for 15 minutes. Slides were rinsed in tap water, mounted, and then examined by light microscopy (Nikon Eclipse90i).

Guaiacol quantification in tissues. Mice were treated with 360 mg/kg guaiacol via oral gavage supplied with 50% guaiacol in glycerol. Mice were sacrificed by CO_2 asphyxiation and cervical dislocation. Tissues were collected and weighed to prepare 10% wet tissue isopropanol extracts.

Guaiacol was quantified by spectrophotometry at 500 nm after its oxidation. The absorbance of 500-nm light by guaiacol increases upon oxidation and allows its spectrophotometric detection. Briefly, guaiacol was extracted from 10 mg tissue in a glass-glass homogenizer using 100 μl isopropanol. Twenty microliters of extract was mixed with 80 μl oxidation reaction mix composed of 1 μg/ml horseradish peroxidase (Thermo Fisher Scientific) and 1 mM hydrogen peroxide (final concentrations for the total volume of 100 μl). Guaiacol standards were generated from 25 mM guaiacol stock solution prepared and diluted in isopropanol. The reaction mixture was kept for 5 minutes at 37°C for color development and absorbance was measured in the BioTek Powerwave HT Microplate Reader spectrophotometer.

Glucose tolerance testing. Mice from control and GBE-deficient groups were fasted for 16 hours. D-Glucose (1.2 mg/g weight) was injected into the peritoneum of conscious mice. Blood was obtained from the tail at 0, 10, 40, 100, and 180 minutes after injection, and the glucose concentration was determined with a glucose meter (Glucometer Elite, Bayer).

Statistics. A P value of 0.05 or below was considered significant. All statistical analysis was done for at least $n = 3$ repetitions. Multiple comparisons to control were computed by 1-way ANOVA with Dunnet's post hoc test. Paired comparisons were performed by Student's t test and differences between kinetic parameters (K_m and V_{max}) were confirmed by the extra-sum-of-squares F test.

Study approval. The studies were approved by the Columbia University Institutional Animal Care and Uses Committee (IACUC) and in accordance with the Institute for Laboratory Animal Research (ILAR) guide for care and use of laboratory animals.

Author contributions

OK and HOA wrote the manuscript, designed research, conducted experiments, analyzed data, and supervised research. IF, LJS, NK, RA, DY, and SP conducted experiments and analyzed data. AL read the manuscript and provided comments. MW, HS, PE, and WWY supervised research.

Acknowledgments

This work wassupported by funds provided by the Adult Polyglucosan Body Disease Research Foundation (to OK and HOA), the Keith B. Hayes Research Foundation (to HOA), the Israel Ministry of Science grant number 3-14355 (to OK and MW), and gifts from Gayle and Robert Lipsig, and from Robert Fram (to HOA). We would like to acknowledge and thank Berge Minassian and Erin Chown for sharing their results on Ptg knockdown with us. This work is dedicated to the memory of Mr. Gregory Weiss, founder and former president of the Adult Polyglucosan Body Disease Research Foundation.

Address correspondence to: Hasan Orhan Akman, 630W 168th street room 4-431, New York, New York 10032, USA. Phone: 55.126.55401; Email: hoa2101@cumc.columbia.edu. Or to: Or Kakhlon, Department of Neurology, Hadassah-Hebrew University Medical Center, Ein Kerem, Jerusalem 91120, Israel. Phone: 972.54.6812380 Email: ork@hadassah.org.il.

1. Minassian BA. Post-modern therapeutic approaches for progressive myoclonus epilepsy. *Epileptic Disord*. 2016;18(S2):154–158.
2. Minassian BA, et al. Mutations in a gene encoding a novel protein tyrosine phosphatase cause progressive myoclonus epilepsy. *Nat Genet*. 1998;20(2):171–174.
3. Tagliabracci VS, et al. Abnormal metabolism of glycogen phosphate as a cause for Lafora disease. *J Biol Chem*. 2008;283(49):33816–33825.
4. Robitaille Y, Carpenter S, Karpati G, DiMauro SD. A distinct form of adult polyglucosan body disease with massive involvement of central and peripheral neuronal processes and astrocytes: a report of four cases and a review of the occurrence of polyglucosan bodies in other conditions such as Lafora's disease and normal ageing. *Brain*. 1980;103(2):315–336.
5. Hedberg-Oldfors C, Oldfors A. Polyglucosan storage myopathies. *Mol Aspects Med*. 2015;46:85–100.
6. Pederson BA, et al. Inhibiting glycogen synthesis prevents Lafora disease in a mouse model. *Ann Neurol*. 2013;74(2):297–300.
7. Turnbull J, et al. Lafora disease. *Epileptic Disord*. 2016;18(S2):38–62.
8. Pederson BA, Chen H, Schroeder JM, Shou W, DePaoli-Roach AA, Roach PJ. Abnormal cardiac development in the absence of heart glycogen. *Mol Cell Biol*. 2004;24(16):7179–7187.
9. Fong NM, Jensen TC, Shah AS, Parekh NN, Saltiel AR, Brady MJ. Identification of binding sites on protein targeting to glycogen for enzymes of glycogen metabolism. *J Biol Chem*. 2000;275(45):35034–35039.
10. Turnbull J, et al. PTG depletion removes Lafora bodies and rescues the fatal epilepsy of Lafora disease. *PLoS Genet*. 2011;7(4):e1002037.
11. Turnbull J, et al. PTG protein depletion rescues malin-deficient Lafora disease in mouse. *Ann Neurol*. 2014;75(3):442–446.
12. Kollberg G, et al. Cardiomyopathy and exercise intolerance in muscle glycogen storage disease 0. *N Engl J Med*. 2007;357(15):1507–1514.
13. Orho M, et al. Mutations in the liver glycogen synthase gene in children with hypoglycemia due to glycogen storage disease type 0. *J Clin Invest*. 1998;102(3):507–515.
14. Nammack CH, Tiber AM. The treatment of lung abscess by means of Guaiacol intravenously. *JAMA*. 1937;109(5):330–336.
15. Heatley RV, Evans BK, Rhodes J, Atkinson M. Guaiacol -- a new compound in the treatment of gastro-oesophageal reflux? *Gut*. 1982;23(12):1044–1047.
16. Orhan Akman H, et al. A novel mouse model that recapitulates adult-onset glycogenosis type 4. *Hum Mol Genet*. 2015;24(23):6801–6810.
17. Akman HO, Sheiko T, Tay SK, Finegold MJ, Dimauro S, Craigen WJ. Generation of a novel mouse model that recapitulates early and adult onset glycogenosis type IV. *Hum Mol Genet*. 2011;20(22):4430–4439.
18. Skurat AV, Dietrich AD, Roach PJ. Glycogen synthase sensitivity to insulin and glucose-6-phosphate is mediated by both NH2- and COOH-terminal phosphorylation sites. *Diabetes*. 2000;49(7):1096–1100.
19. Suter M, Riek U, Tuerk R, Schlattner U, Wallimann T, Neumann D. Dissecting the role of 5'-AMP for allosteric stimulation, activation, and deactivation of AMP-activated protein kinase. *J Biol Chem*. 2006;281(43):32207–32216.
20. Bouskila M, et al. Allosteric regulation of glycogen synthase controls glycogen synthesis in muscle. *Cell Metab*. 2010;12(5):456–466.
21. Jiang S, et al. Starch binding domain-containing protein 1/genethonin 1 is a novel participant in glycogen metabolism. *J Biol Chem*. 2010;285(45):34960–34971.
22. Vilchez D, et al. Mechanism suppressing glycogen synthesis in neurons and its demise in progressive myoclonus epilepsy. *Nat Neurosci*. 2007;10(11):1407–1413.
23. Martić-Kehl MI, Schibli R, Schubiger PA. Can animal data predict human outcome? Problems and pitfalls of translational animal research. *Eur J Nucl Med Mol Imaging*. 2012;39(9):1492–1496.
24. Kakhlon O, et al. Polyglucosan neurotoxicity caused by glycogen branching enzyme deficiency can be reversed by inhibition of glycogen synthase. *J Neurochem*. 2013;127(1):101–113.
25. Ashe KM, et al. Inhibition of glycogen biosynthesis via mTORC1 suppression as an adjunct therapy for Pompe disease. *Mol Genet Metab*. 2010;100(4):309–315.
26. Solmesky LJ, et al. A novel image-based high-throughput screening assay discovers therapeutic candidates for adult polyglucosan body disease. *Biochem J*. 2017;474(20):3403–3420.
27. Ogata N, Matsushima N, Shibata T. Pharmacokinetics of wood creosote: glucuronic acid and sulfate conjugation of phenolic compounds. *Pharmacology*. 1995;51(3):195–204.
28. Bachmanov AA, Reed DR, Beauchamp GK, Tordoff MG. Food intake, water intake, and drinking spout side preference of 28 mouse strains. *Behav Genet*. 2002;32(6):435–443.
29. Lesk AM, Chothia C. How different amino acid sequences determine similar protein structures: the structure and evolutionary dynamics of the globins. *J Mol Biol*. 1980;136(3):225–270.